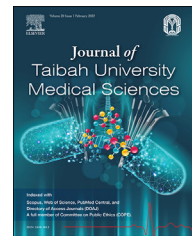




# Taibah University

## Journal of Taibah University Medical Sciences

www.sciencedirect.com



### Original Article

## *In silico* screening of *Hippophae rhamnoides* polyphenols targeting the RhoA protein as a potential liver cancer treatment



Rukhsana Tabassum, MS and Erum Dilshad, PhD \*

Department of Bioinformatics and Biosciences, Faculty of Health and Life Sciences, Capital University of Science and Technology (CUST), Islamabad, Pakistan

Received 5 July 2024; revised 21 October 2024; accepted 25 January 2025; Available online 13 February 2025

### المخلص

**أهداف البحث:** نظرا لارتباط اشارات بروتينات "آر اتش أو جي تي بيز" المضطربة بسرطانات متعددة، يمكن بحثها كهدف محتمل لعلاجات سرطان الكبد. تعتبر نبتة العليق البحري من النباتات الطبية المهمة الموجودة في جبال قراقرم. ويعتقد باحتوائها على مركبات متعددة الفينول قادرة على تثبيط بروتين "آر اتش أو - أ"، مما قد يوفر تأثيرات مضادة لسرطان الكبد.

**طرق البحث:** تم تحديد المركبات متعددة الفينول في المستخلص الميثانولي للعليق البحري باستخدام التحليل الكروماتوغرافي السائل عالي الكفاءة ثم فحصها للتحري عن امكانياتها المضادة للسرطان عبر الارساء الجزيئي ومحاكاة الديناميكا الجزيئية ضد بروتين "آر اتش أو - أ". تم تحديد قيم الانحراف المتوسط الجذري التربيعي وقيم ثقل الجذر المتوسط المربع لكل مركب مختار، تبعها تحليل خصائص الامتصاص والتوزيع والتمثيل الغذائي والإفراز والسمية.

**النتائج:** وجدت المركبات متعددة الفينول حمض الغاليك وحمض الساليسيليك وحمض الكافيك والكيمفيرول والروتين والكيرستين والكومارين وحمض الفيروليك وحمض السينابيك وحمض النيق وحمض الفانيليك وحمض الكلوروجينيك في المستخلص الميثانولي للعليق البحري. بناء على قاعدة لينسكي الخماسية ودرجة فينا وحجم التجويف، تم اختيار خمسة روابط لمزيد من البحث حيث تظهر خصائص ملحوظة. وفقا لذلك، تبين حمض الكافيك كمركب بارز مع خصائص امتصاص وتوزيع وتمثيل غذائي وطرح وسمية جذابة ودرجة ارساء ونتائج محاكاة ديناميكية جزيئية مثالية.

**الاستنتاجات:** نظرا لبقائه سليما وارتباطه ببنية البروتين طوال فترة المحاكاة، مما يدل على تفاعل قوي بين البروتين والرابط ويشير لتأثير تثبيطي محتمل، قد يمتلك حمض الكافيك القدرة العظمى على تثبيط بروتين "آر اتش أو - أ".

وبالتالي، مطلوب مزيد من البحث لدراسة حمض الكافيك كخيار دوائي محتمل للتطوير الدوائي المستقبلي.

**الكلمات المفتاحية:** اكتشاف الدواء؛ العليق البحري؛ المحاكاة الحاسوبية؛ سرطان الكبد؛ الارساء الجزيئي؛ محاكاة الديناميكا الجزيئية؛ متعددات الفينول؛ الفحص الكيميائي النباتي؛ حركة الدواء؛ بروتين "آر اتش أو - أ"

### Abstract

**Objective:** Because aberrant Rho GTPase signaling has been associated with multiple cancers, it was investigated as a potential target for liver cancer treatment drugs. The important medicinal plant *Hippophae rhamnoides*, found in the Karakoram Mountains, is believed to contain polyphenols that inhibit RhoA protein, thus potentially eliciting effects against liver cancer.

**Methods:** Polyphenols were identified in the methanolic extract of *H. rhamnoides* with HPLC, then screened for their anticancer potential against the RhoA protein through molecular docking and molecular dynamic simulations. The RMSD and RMSF values for each selected compound were determined, and ADMET characteristics were analyzed.

**Results:** The polyphenols gallic acid, salicylic acid, caffeic acid, kaempferol, rutin, quercetin, coumarin, ferulic acid, sinapic acid, HB acid, vanillic acid, and chlorogenic acid were found in the methanolic extract of *H. rhamnoides*. On the basis of Lipinski's rule of five, the Vina score, and the cavity size, we chose five ligands with favorable features for further research. Caffeic acid was the most promising compound, on the basis of favorable ADMET qualities, and the best docking score and MD simulation results.

**Conclusion:** Caffeic acid remained intact and bound the protein structure throughout the simulation run, thus demonstrating a robust interaction between the protein

\* Corresponding address:

E-mail: [dr.erum@cust.edu.pk](mailto:dr.erum@cust.edu.pk) (E. Dilshad)

Peer review under responsibility of Taibah University.



Production and hosting by Elsevier

and ligand, and indicating a possible inhibitory effect. Therefore, this compound might have the greatest ability to inhibit the RhoA protein. Further research is required to examine caffeic acid as a potential medication option for future drug development.

**Keywords:** Drug discovery; *H.rhamnoides*; Liver cancer; Phytochemical screening; Polyphenols; RhoA protein

© 2025 The Authors. Published by Elsevier B.V. This is an open access article under the CC BY-NC-ND license (<http://creativecommons.org/licenses/by-nc-nd/4.0/>).

## Introduction

Liver cancer is a worldwide health concern that is becoming increasingly common. By 2025, 1 million people are expected to be affected by liver cancer annually.<sup>1</sup> Mutations and epigenetic changes are the root causes of cancer. Normal cells have a basic ability to develop into neoplasias, which acquire characteristics such as unchecked growth, angiogenesis, and resistance to cell death. Hanahan and Weinberg have researched several important malignant cell characteristics, known as hallmarks of cancer, including the ability to evade immune cells, alter metabolism, disrupt the genome, and induce inflammation and consequently support tumor growth.<sup>2,3</sup>

Hepatocellular carcinoma (HCC) is the most common type of liver cancer, accounting for more than 90 % of cases. The primary risk factor for HCC is the hepatitis B virus, which is responsible for more than 50 % of cases. Liver cancer is among the top five most lethal and fast growing cancers.<sup>4</sup> Liver illnesses are typically more common in developing than developed countries. Hepatitis B, hepatitis C, fatty liver disorders, liver cirrhosis associated with alcohol use, smoking, overweight, diabetes, and excess iron in certain diets are risk factors for liver cancer.<sup>5</sup> The disease has a dismal prognosis; only 5–15 % of individuals are eligible for surgical removal, and even then, this treatment is appropriate only in early stages of the condition.<sup>6</sup>

Small G proteins called Rho GTPases regulate the cytoskeleton, polarity, morphology, vesicular motions, the cell cycle, cell destruction, and gene expression in cells.<sup>7</sup> Numerous investigations have shown indicated that these small proteins actively contribute to cancer development. Consequently, Rho GTPases might serve as new targets for cancer biology research. Cancers exhibit notable alterations at the cell level during spread and progression. The most frequent alteration is tumor growth due to aberrant Rho GTPase signaling.<sup>8</sup> Rho GTPases are involved in cell functions and are associated with all stages of cancer growth and progression, such as angiogenesis, apoptotic resistance, invasion of tissues, and metastasis in HCC.<sup>9</sup> Therefore, determining how Rho GTPases function in HCC may aid in the search for treatments for this severe cancer. Although dysregulation of RhoA has been studied in HCC, limited studies have investigated natural inhibitors of this protein. Bioinformatics tools, such as molecular docking and molecular dynamics (MD) simulation, may contribute

to innovations in drug candidates for liver cancer with minimal adverse effects. Some studies have indicated that small molecule inhibitors might serve as a potential approach to therapeutically target RhoA in the future.<sup>10</sup>

Since the dawn of time, humans have relied on the therapeutic qualities of plants. Most chemotherapy drugs are made synthetically or are made of substances refined from plants. Herbal therapy is a useful substitute for traditional cancer care. Numerous investigations have been conducted on naturally occurring substances with cytotoxic properties that might potentially kill cancer cells. Because of these benefits, medicinal plants have been studied and used to develop anti-cancer medications. Research on plant bioactive chemicals as potential anticancer agents has recently gained increased attention.<sup>11</sup> Plant phytochemicals fight cancer through processes such as promoting DNA repair, increasing the synthesis of beneficial enzymes that boost immunity, and inducing antioxidants.<sup>12</sup>

*Hippophae rhamnoides* is a shrub belonging to the Elaeagnaceae family. Its fruits are nutrient dense, containing vitamins and minerals, and are used extensively in the pharmaceutical and cosmetics industries. The berries, often called seaberrries, contain distinctive bioactive ingredients including phytosterols such as beta-sitosterol, unsaturated fatty acids, vitamins (particularly vitamins C and E), phenolic compounds,  $\beta$ -carotene, lycopene, phytosterols, polyunsaturated fatty acids (particularly omega 7 palmitoleic acid), minerals (e.g., iron and calcium), and amino acids.<sup>13</sup> The berries' anti-inflammatory, antioxidant, and anticancer properties have been researched in the forms of juice, jam, and oil. Fruit size, maturity, composition, and storage and processing methods all affect the concentrations of chemicals present.<sup>14</sup>

*In silico* prediction with computer-stimulated models can aid in developing biomedicines and understanding the pharmacology of possible treatments. Molecular docking has grown in importance as a component of *in silico* drug-creation processes in recent years. The interactions between biomolecules and small molecules determined with this method can enhance understanding of binding sites and affinities, as well as mechanisms of action. Therefore, molecular docking is a widely accepted method in the drug-design process.<sup>15,16</sup> Additionally, *in silico* techniques can aid in identifying specific proteins that are targeted by molecules and mediate anticancer activity, as well as in tracing specific active metabolites. This study's primary goal was to use molecular docking to determine the interactions between the polyphenols (obtained through HPLC) identified from the methanolic extracts of *H. rhamnoides* and the RhoA protein.

## Methods

### Collection and preparation of plant material

Specific regions of Gilgit Baltistan, including the Ghizer district, parts of the Skardu division, and central and upper Hunza, were targeted for the collection of flora. The chosen plant was identified with the specimen voucher number FR-01 for *H. rhamnoides* from the herbarium of Hazara University of Pakistan. The seeds were first dried at room temperature for 72 h to prepare the plant extract and then were

ground into a powder with a machine grinder. Subsequently, 1 gm powdered seed and 10 mL 80/20 methanol/water solution were combined for the extraction process. After stirring of the mixture for 2 min, each extract was centrifuged for 30 min at 5000 rpm. A rotatory evaporator was then used to evaporate the methanolic extract. To the extract retained after evaporation, 2 mL acetonitrile was added, and extraction was performed three times with 1 mL hexane. The acetonitrile fraction was subsequently dried, and 2 mL methanol was added to this dried fraction. The extracted material was then subjected to HPLC analysis to identify the phenolic components. Similarly, standard solutions were prepared by dissolution of 100 mg powdered seed in 1 mL methanol.<sup>17</sup>

#### *Quantitative analysis of polyphenols with HPLC chromatography*

A Perkin Elmer Flexar System, including an internal degasser, a diode matrix detector, and an Eclipse ODS Hypersil C18 column (15 cm), was used for the HPLC analysis. Solvent 1 (water/formic acid, 0.10 %) and solvent 2 (acetonitrile/formic acid, 0.10 %) composed the mobile phase. The injection volume was 20  $\mu$ L, and the flow rate was 1 mL/min. To prevent damage to the column, further safety measures were implemented while the extracts and standards were carefully filtered through Millipore membranes. For identification of the peaks, retention times were compared with standards. A computer program was used to view the signals that the detector recorded.<sup>18</sup> The analytes were determined on the basis of specified retention times (Table 1).

#### *Protein selection, refinement, and functional domain identification*

The UniProt database (<http://www.uniprot.org/uniprotkb/entry>) was used to acquire the RhoA target protein's main sequence in FASTA format (<http://www.ncbi.nlm.nih.gov/gene>). The ProtParam tool (<https://web.expasy.org/protparam>) was used to predict its characteristics, positively and negatively charged amino acids, molecular weight, instability index, and theoretical PI, and physical and chemical properties.<sup>19</sup> RhoA's final 3D structure was obtained in PDB format from the Protein Data Bank (<http://www.rcsb.org/structure>). PyMOL (<http://pymol.org/pymol-command-ref>) software was used to refine the protein structure.<sup>20</sup> The online database Interpro (<http://www.ebi.ac.uk/interpro>) was used to identify target protein functional domains. Additionally, MODELLER v10.5 (<https://salilab.org/modeller/>) was used to model previously unmodeled residues in the structure. The generated protein structure was applied to additional examination of molecular docking.

#### *Ligand preparation and molecular docking*

The HPLC-identified polyphenols of *H. rhamnoides* were obtained from the PubChem database (<http://pubchem.ncbi.nlm.nih.gov>).<sup>19</sup> The Chem Pro ultra program (<http://chemistrydocs.com/chemdraw-ultra-12-0>) (chem 3D

v12.0.2) was used to minimize the energy consumption of these specific ligands. This stage in the ligand preparation process was crucial, because unstable ligands exhibited inconsistent Vina scores after docking. Additionally, the drug likeliness of the chosen ligands from the PubChem database and the conventional medication sorafenib, which is used to treat liver cancer, was examined. The ligands chosen for this investigation underwent testing for Lipinski's rule of five, to determine their drug likeness. ADMET characteristics were also examined, to evaluate the molecules as possible drug sources and to facilitate the drug discovery process. The online program PKCSM (<http://biosig.lab.uq.edu.au/pkcsm/prediction>) was used for drug screening according to drug score, toxicity, and drug likeliness.<sup>20</sup> Ligplot Plus software (version v.1.4.5) (<https://www.ebi.ac.uk/thornton-srv/software/LigPlus/>) was used to produce a diagram of protein-ligand interactions. Ligplot Plus was applied to examine the hydrophobic interactions and hydrogen bonds of particular docked molecules, and calculate the root mean square deviation (RMSD) values. To determine the RMSD, we used UCSF Chimera (<http://www.cgl.ucsf.edu/chimera>).

For molecular docking, we used CB dock Yang Cao Lab (<http://clab.labshare.cn/cb-dock>), an online docking tool that automatically finds binding sites, simplifies docking procedures, and improves accuracy by predicting target protein binding sites.<sup>21</sup> This tool shows results in five different poses in 3D visualization. We selected the best pose with the lowest Vina score. Three parameters were considered in docking—Vina score, cavity size, and grid map size—to aid in analysis of docking outcomes. The molecular docking results were analyzed with the Vina score, which indicated the binding affinity between the selected protein and ligands. The Vina score represents various interaction types such as hydrogen bonding, hydrophobic interactions, and other steric binding forces. These particular interactions were calculated and adjusted according to the number of rotatable bonds, regarding entropic penalties associated with molecular flexibility. A lower (more negative) Vina score indicates stronger binding affinity.<sup>22</sup>

The virtual screening of RhoA against the selected ligands (caffeic acid, gallic acid, and salicylic acid) was performed in GNINA (<https://github.com/gnina/gnina>) molecular docking software, by using convolutional neural networks for the scoring function.<sup>23</sup> Moreover, the complexes with the highest binding affinity scores among were shortlisted. Interaction analysis was performed on these shortlisted complexes to identify interacting residues within the domain regions. Additionally, the 2D interactions of these shortlisted complexes were visualized with Discovery Studio Visualizer (Biovia, D. S. (2019) Discovery Studio Visualizer, San Diego).

#### *Molecular dynamics simulation of shortlisted complexes*

To observe the stability and flexibility of the shortlisted complexes, we performed MD simulations in Maestro 12.0 (version 12.0.012, Schrödinger, LLC, New York, NY), a robust MD suite.<sup>24</sup> First, in the protein preparation wizard, the protein was subjected to pre-processing and refinement

along with the removal of water beyond 5 Å. The SPC force field was applied as the solvent model in the system builder module, including salt ions. Subsequently, the system was loaded into the MD window module, in which parameters were configured for 100 ns simulation duration at a default temperature of 300 K. Eventually, the trajectory file generated from the simulation was imported into the simulation interaction diagram module for post-simulation analysis, along with the RMSD and root mean square fluctuations (RMSF) values. Moreover, three parameters were examined to assess ligand properties: solvent accessible surface area (SASA), polar surface area, and radius of gyration. The binding abilities of the molecules were observed throughout the simulation run with snapshots generated after every 100th frame.

## Results and discussion

Using HPLC chromatography, we studied the methanolic extract of *H. rhamnoides*. The HPLC profile of the investigated plant extract was examined with the standard polyphenol retention period. The method relied on comparison of the retention times of the samples versus the standard. The chromatogram (Figure 1A) displays the standards used. This method enabled the identification of 12 polyphenols (Table 1)—coumarin, caffeic acid, gallic acid, quercetin, chlorogenic acid, HB acid, vanillic acid, sinapic acid, ferulic acid, rutin, kaempferol, and salicylic acid—in the extract of *H. rhamnoides* (Figure 1B). Chlorogenic acid had the highest concentration in this extract (1.151 µg/mg). In a previous study determining the phytochemical makeup of *H. rhamnoides* leaves and berries, many polyphenols have been found.<sup>25</sup> We identified the additional polyphenols sinapic acid and salicylic acid. From the current study and earlier studies, we inferred that the berries of *H. rhamnoides* have high polyphenol content, which varies according to climate, growth environment, and genetic background.<sup>26,27</sup>

**Table 1: Polyphenols found in the methanolic extract of *H. rhamnoides* at 275 nm.**

No.	Polyphenols found in <i>H. rhamnoides</i>	Retention time (min)	Concentration (µg/mg)
1	Chlorogenic acid	3.001	1.151
2	Gallic acid	3.335	0.140
3	HB acid	6.972	0.057
4	Caffeic acid	7.398	0.031
5	Vanillic acid	7.642	0.084
6	Kaempferol	11.131	0.215
7	Sinapic acid	12.158	0.029
8	Ferulic acid	12.645	0.022
9	Quercetin	17.161	0.011
10	Salicylic acid	15.396	0.449
11	Rutin	23.504	0.060
12	Coumarin	16.042	0.865

## Protein structure analysis

The primary sequence of the RhoA protein was retrieved from the UniProt database under accession no. P61586 (length: 193 amino acids). The online tool ProtParam ExPASy was used to study the physiochemical properties of RhoA (Table 2). These properties included molecular weight, extension coefficient, instability index, positively and negatively charged amino acids, theoretical PI, and grand average of hydrophobicity (GRAVY).<sup>28</sup>

The 3D structure of the RhoA protein was downloaded in pdb format (Figure 2A) from pdb id 4XH9 in the Protein Data Bank.<sup>29</sup> This protein molecule was used as a target molecule for docking with selected ligands. Rho GTPases are highly conserved enzymes whose dysregulation is associated with a range of abnormal cellular processes; moreover, targeting these proteins has been found to minimize the severity of cancer progression.<sup>30</sup> The structure of the target protein, RhoA, was visualized in PyMOL software (Figure 2 (B)). InterPro, an online database, was used to identify the functional domains of RhoA protein. Conserved domains are involved in sequence/structure/relationships.<sup>31</sup> This protein contains primarily small GTP-binding domains (IPR005225 and TIGR00231) and other domains in the small GTPase Rho family profile (PS51420) (Figure 3).

## Preparation of ligands for molecular docking

The 2D structure and associated data for the ligands found in the plant extract by HPLC were acquired from the PubChem database, as shown in Table 3.<sup>32</sup> Subsequently, the ligand's energy was minimized in ChemPro software (chem12). This step was crucial in preparing the ligand for docking, because unstable ligands might potentially affect the Vina score.

## Molecular docking

Finding the ideal binding conformation between target proteins and ligands is the main goal of molecular docking.<sup>33</sup> We used the online docking tool CB-Dock, which automatically identifies binding sites, to perform docking with the advanced software AutoDock Vina. This method simplified the docking procedures and improved accuracy by predicting target protein binding sites. A 3D visualization of the results in five distinct positions was determined (Figure 4), and the optimal stance with the lowest Vina score was chosen.<sup>34</sup> The molecular docking results were analyzed according to the Vina score, which indicated the binding affinity between the selected protein and ligands. The Vina score represents various interaction types, such as hydrogen bonding, hydrophobic interactions, and other steric binding forces. These interactions were calculated and adjusted according to the number of rotatable bonds, regarding entropic penalties associated with molecular flexibility. A lower (more negative) Vina score indicates stronger binding affinity. Furthermore, the numbers of hydrogen bonds and hydrophobic interactions were determined (Figure 5).

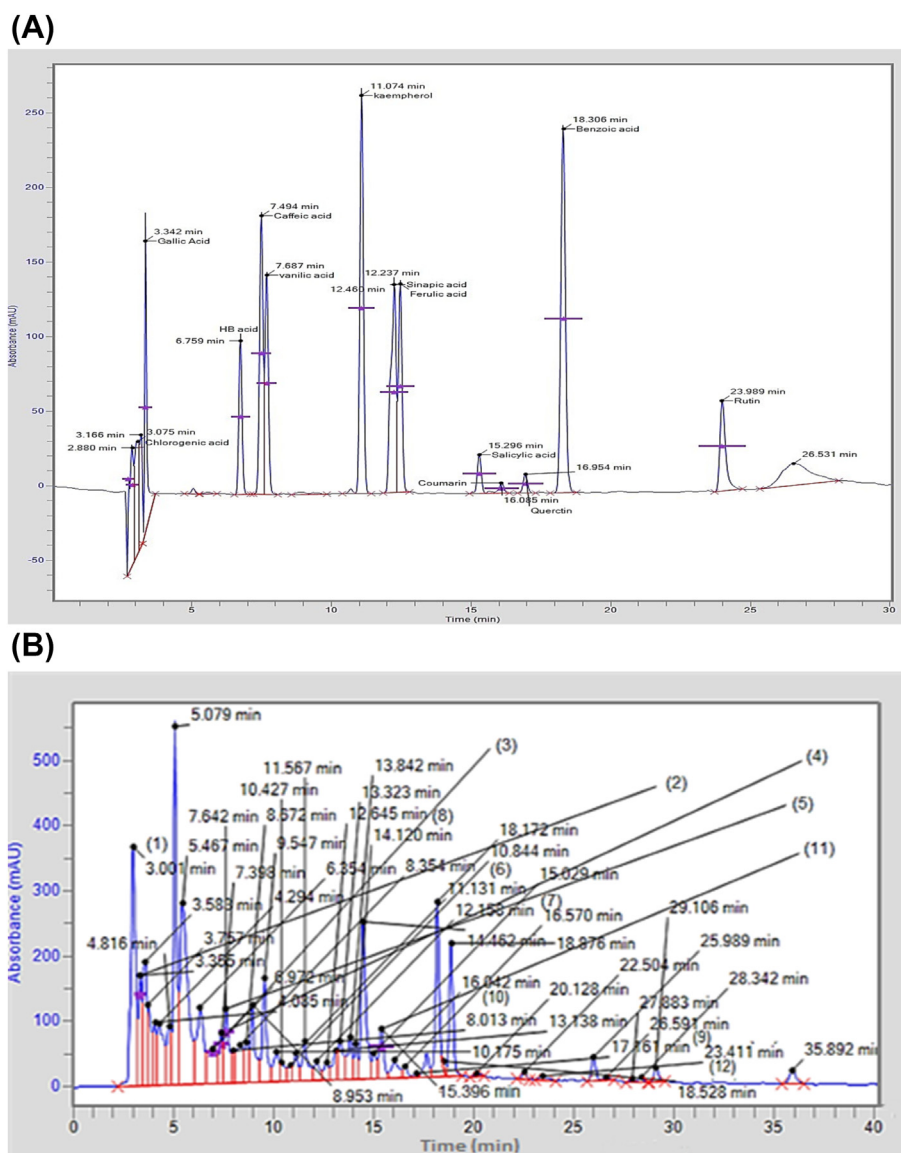


**Figure 1:** (A) Chromatogram of the standard mixture used in HPLC chromatography. The standards comprised chlorogenic acid, gallic acid, HB acid, caffeic acid, vanillic acid, kaempferol, sinapic acid, ferulic acid, quercetin, salicylic acid, benzoic acid, rutin, and coumarin. (B) Chromatogram of the methanolic extract of *H. rhamnoides* at 275 nm. Identified polyphenols are represented as follows: 1, chlorogenic acid; 2, gallic acid; 3, HB acid; 4, caffeic acid; 5, vanillic acid; 6, kaempferol; 7, sinapic acid; 8, ferulic acid; 9, quercetin; 10, salicylic acid; 11, rutin; and 12, coumarin.

In selecting the five polyphenols, we considered docking parameters such as the Vina score, cavity size, and grid map; we also considered whether the selected ligands followed Lipinski's rule of five, because ligands meeting the rule are likely to be readily absorbed. Some ligands had an ideal Vina score but did not follow Lipinski's rule, because their molecular weights exceeded 500 Da. Likewise, some ligands had

low grid map scores, whereas a high grid map score indicates strong interactions. Moreover, the cavity size should be large, but not too large, for small molecules. Considering factors such as the optimal vina score, cavity size, grid map score, and Lipinski's rule of five (Table 4 and Table 5), we selected the ligands quercetin, gallic acid, kaempferol, salicylic acid, and caffeic acid in the *H. rhamnoides* extract.

**Table 2: Physicochemical properties of RhoA protein, studied with the ProtParam tool.**

Number of amino acids	Molecular weight	Instability index (II)	Extension coefficient 1	Extension coefficient 2	Theoretical PI	Positively charged particles	Negatively charged particles	GRAVY
193	5.83	51.73	18825	18450	5.83	29	31	-0.36

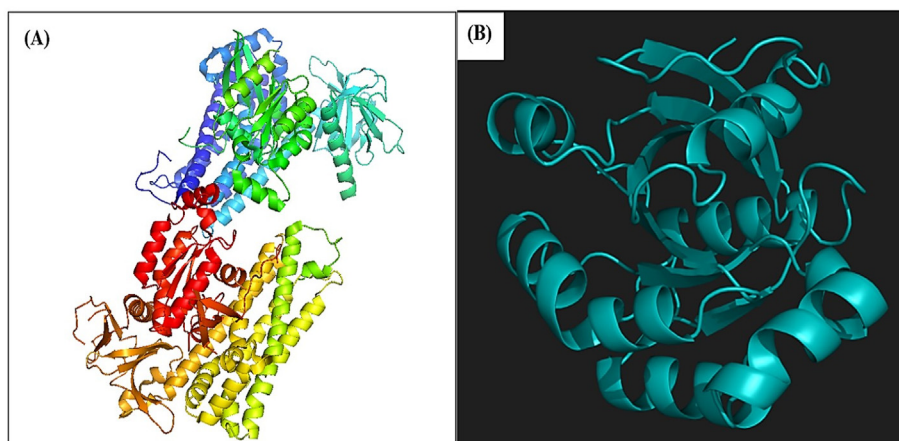


**Figure 2:** (A) 3D structure of RhoA protein retrieved from the Protein Data Bank. (B) RhoA protein visualized with PyMOL.

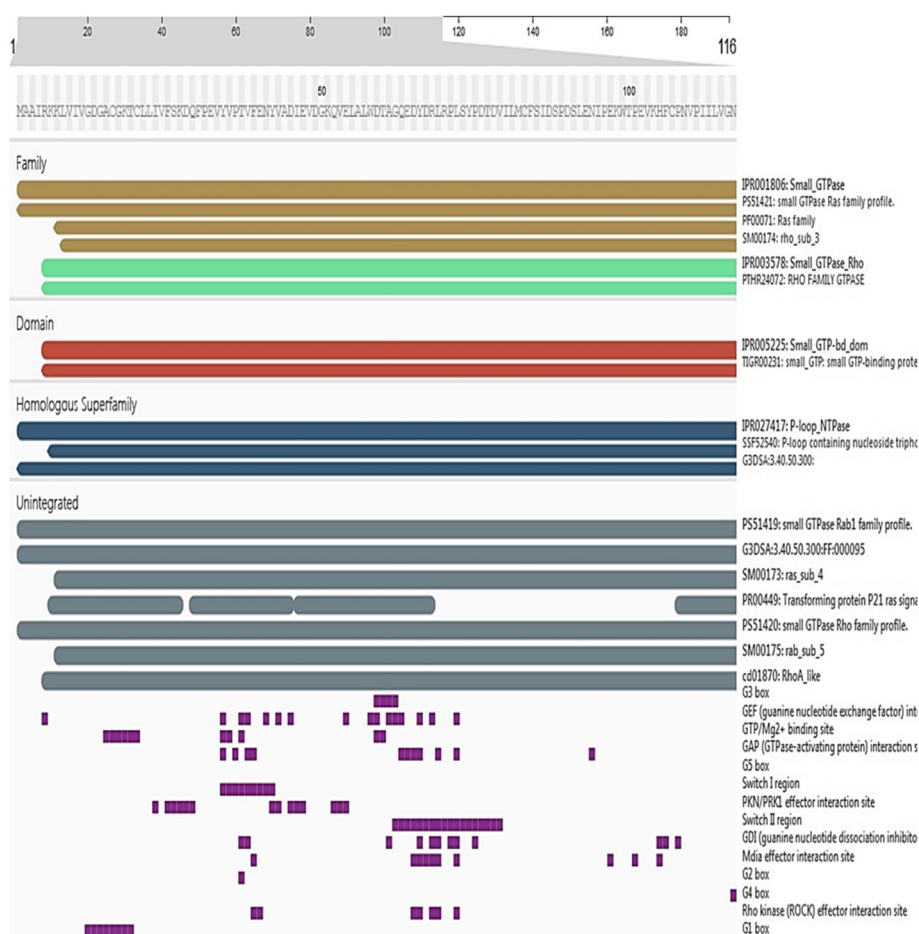


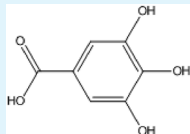
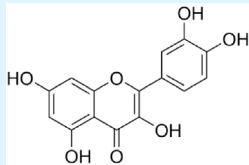
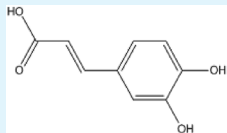
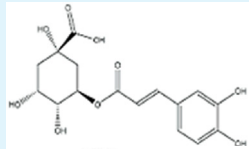
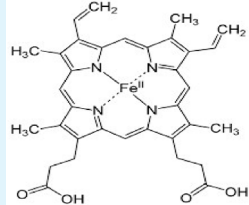
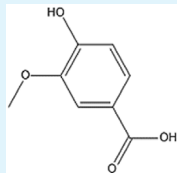
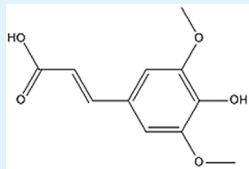
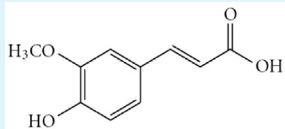
**Figure 3:** RhoA protein, with functional domains identified with Interpro.

Sorafenib, a synthetic drug used to treat liver cancer, was also used to compare ligand interactions with the target protein.

Next, we used UCSF Chimera software to examine the RMSD values in the docking results (Figure 6 and Table 6). The RMSD values expected from interaction outcomes were

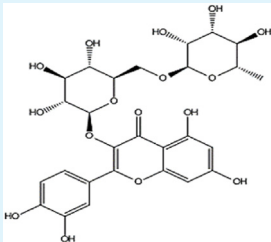
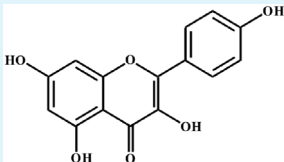
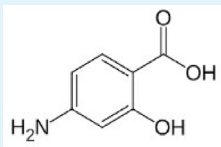
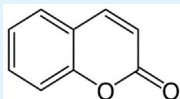
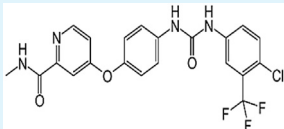
used to quantify the system's deviation from its initial conformation and to analyze variations in docking poses. The average distance between the atoms in a protein and overlaid ligand structure was determined according to the RMSD.<sup>35</sup> All poses in the current study were considered ideal for illustrating the RMSD rules. The optimal

**Table 3: Identified ligands and related information.**

No.	Ligands	CID No.	Molecular formula	Molecular weight (g/mol)	Ligand 2D structure
2	Gallic acid	370	C <sub>7</sub> H <sub>6</sub> O <sub>5</sub>	170.12	
9	Quercetin	5280343	C <sub>15</sub> H <sub>10</sub> O <sub>7</sub>	302.23	
4	Caffeic acid	689043	C <sub>9</sub> H <sub>8</sub> O <sub>4</sub>	180.15	
1	Chlorogenic acid	1794427	C <sub>16</sub> H <sub>18</sub> O <sub>9</sub>	354.31	
3	HB acid	13285535	Hb	614.16	
5	Vanillic acid	8468	C <sub>8</sub> H <sub>8</sub> O <sub>4</sub>	168.14	
7	Sinapic acid	637775	C <sub>11</sub> H <sub>12</sub> O <sub>5</sub>	224.21	
8	Ferulic acid	445858	C <sub>10</sub> H <sub>10</sub> O <sub>4</sub>	184.18	

(continued on next page)

**Table 3** (continued)

No.	Ligands	CID No.	Molecular formula	Molecular weight (g/mol)	Ligand 2D structure
11	Rutin	5280805	C <sub>27</sub> H <sub>30</sub> O <sub>16</sub>	610.52	
6	Kaempferol	5280863	C <sub>15</sub> H <sub>10</sub> O <sub>6</sub>	286.23	
10	Salicylic acid	338	C <sub>7</sub> H <sub>6</sub> O <sub>3</sub>	138.12	
12	Coumarin	323	C <sub>9</sub> H <sub>6</sub> O <sub>2</sub>	146.14	
	Sorafenib	216239	C <sub>21</sub> H <sub>16</sub> ClF <sub>3</sub> N <sub>4</sub> O <sub>3</sub>	464.83	

positions for salicylic acid, quercetin, gallic acid, kaempferol, and caffeic acid are shown in Table 6, with poses 2, 3, 3, 4, and 2, respectively. Additionally, the RMSF indicated the average residual deviations and provided information on protein flexibility. We required the RMSD values not to exceed 4. An appropriate range for globular proteins is between 1 and 3 Å.<sup>36</sup>

#### Bioactivity analysis of ligands and measurement of ADMET properties

Five ligands and one standard medication were chosen from the drugBank database to assess the ADMET characteristics and analyze the bioactivity of the ligands (Table 7). The selected ligands were required to adhere to Lipinski's rule of five, which indicates the likelihood of serving as an oral medication in humans.<sup>37</sup> This rule states that compounds must meet certain requirements, particularly a log P-value <5. Other requirements are that the molecular weight of the specific chemical must be <500 Da, that no more than five hydrogen bond donors must be present, and that no more than ten hydrogen acceptors must be present.

Ligands meeting Lipinski's rule are likely to be readily absorbed by and bioavailable to the human body.<sup>38</sup>

The pharmacokinetic characteristics of the chosen ligands were investigated in greater detail. The ADMET characteristics (distribution, metabolism, excretion, absorption, and toxicity) are crucial in determining whether a molecule is a good candidate for a medication. The PKCSM tool was used to determine the pharmacokinetic characteristics of the ligands selected as therapeutic candidates and to investigate the ADMET features.<sup>39</sup> On the basis of absorption properties (Table 7), we observed variations in drug and ligand water solubility. For a drug to be effective, it must dissolve in body fluids, such as blood or plasma, which are water based. Good solubility in water indicates that a compound can be easily absorbed into the bloodstream. In this study, the reference drug was less soluble in water than the five selected ligands. Salicylic acid, caffeic acid, and gallic acid were slightly more soluble in water than the other ligands. Similarly, skin permeability is crucial for drugs delivered through the skin. Compounds with lower skin permeability values than the normal threshold (log Kp ≥ -2.50 cm/s) indicate limited skin permeability.<sup>40</sup> The

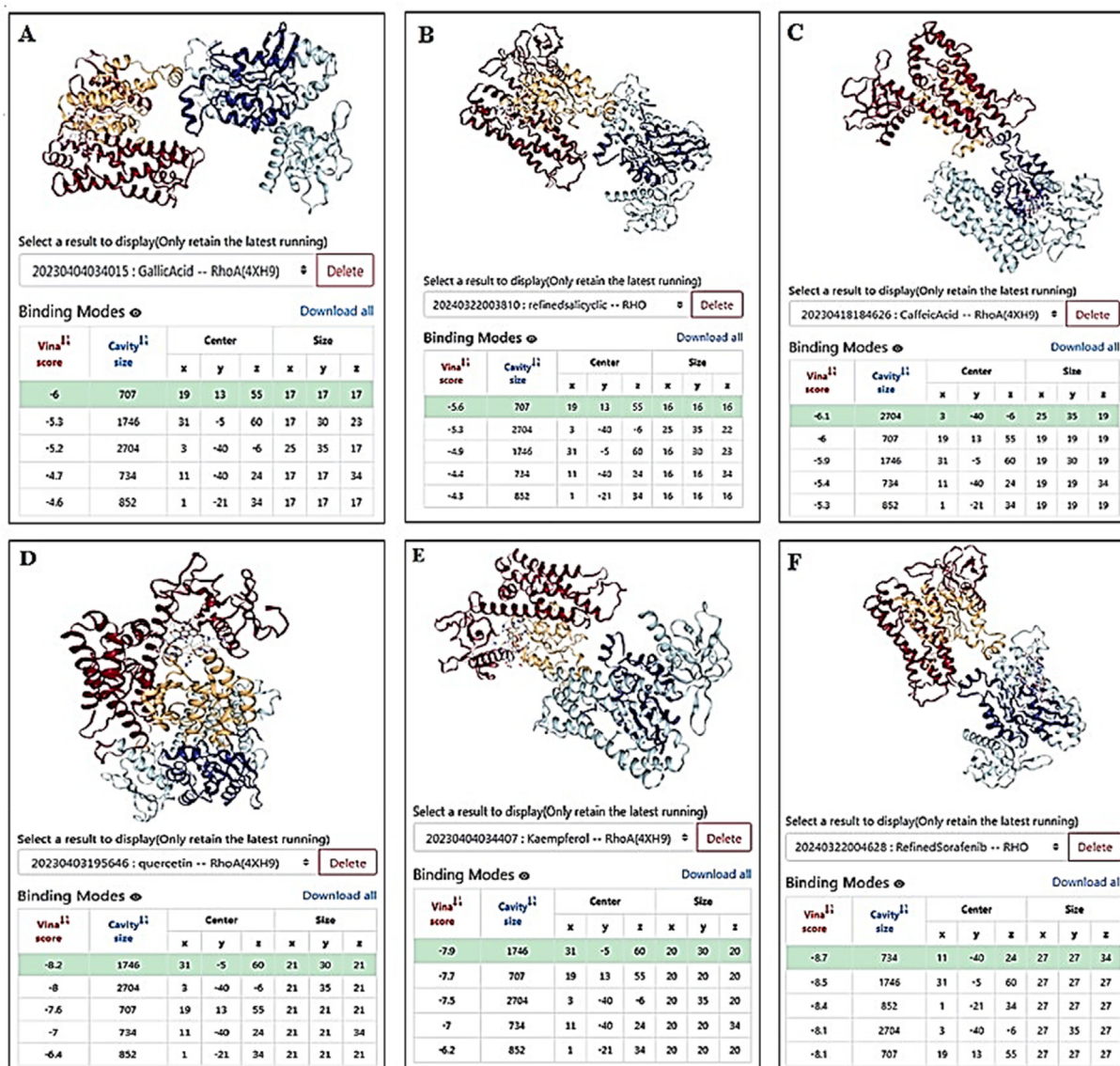


**Figure 4:** Best 3D visualization of conformational poses of the interaction between the target protein and selected ligands. A presents the interaction between gallic acid and RhoA; B presents the interaction between salicylic acid and RhoA; C presents the interaction between caffeic acid and RhoA; D presents the interaction between quercetin and RhoA; E presents the interaction between kaempferol and RhoA; and F presents the interaction between sorafenib and RhoA.

selected compounds showed moderate skin permeability. Investigation of absorption features indicated that some ligands had slightly higher Caco-2 permeability than the synthetic drug. Quercetin and caffeic acid had higher Caco-2 permeability than any other lead molecules. Whereas caffeic acid is not a P-gp substrate and is not an inhibitor of either P-gp I or P-gp II, the synthetic medication sorafenib is a P-gp substrate, P-gp I inhibitor, and non-inhibitor of P-gp II. Similarly, quercetin is a substrate of P-gp, but does not inhibit P-gp I or II. The remaining lead compounds were all non-inhibitors of P-gp I and II, except kaempferol, which is a P-gp substrate. Likewise, high intestinal absorption indicates that a ligand of interest is likely to be absorbed in the gastrointestinal tract after oral intake. In this study, almost all selected ligands showed considerable intestinal absorption, but salicylic acid showed the highest absorption.

Examination of the distribution properties indicated that the CNS permeability of sorafenib was in the region of  $-2$ , whereas other selected ligands, such as caffeic acid, had CNS permeability in the range of  $-2$ . Moreover, salicylic acid, quercetin, and gallic acid had CNS permeabilities in the range of  $-3$ . For other selected ligands, such as kaempferol, the range of CNS permeability was also  $-2$ . Similarly, examination of the unbound fraction in human plasma indicated that several substances had greater values than manufactured drugs. This finding was particularly true for caffeic acid, gallic acid, and salicylic acid. Thus, traditional ligands such as salicylic acid, gallic acid, and caffeic acid were more effective than synthesized drugs. Furthermore, a key aspect in the investigation of ADMET properties is drug metabolism. The synthetic medication sorafenib, as well as the selected ligands salicylic acid,

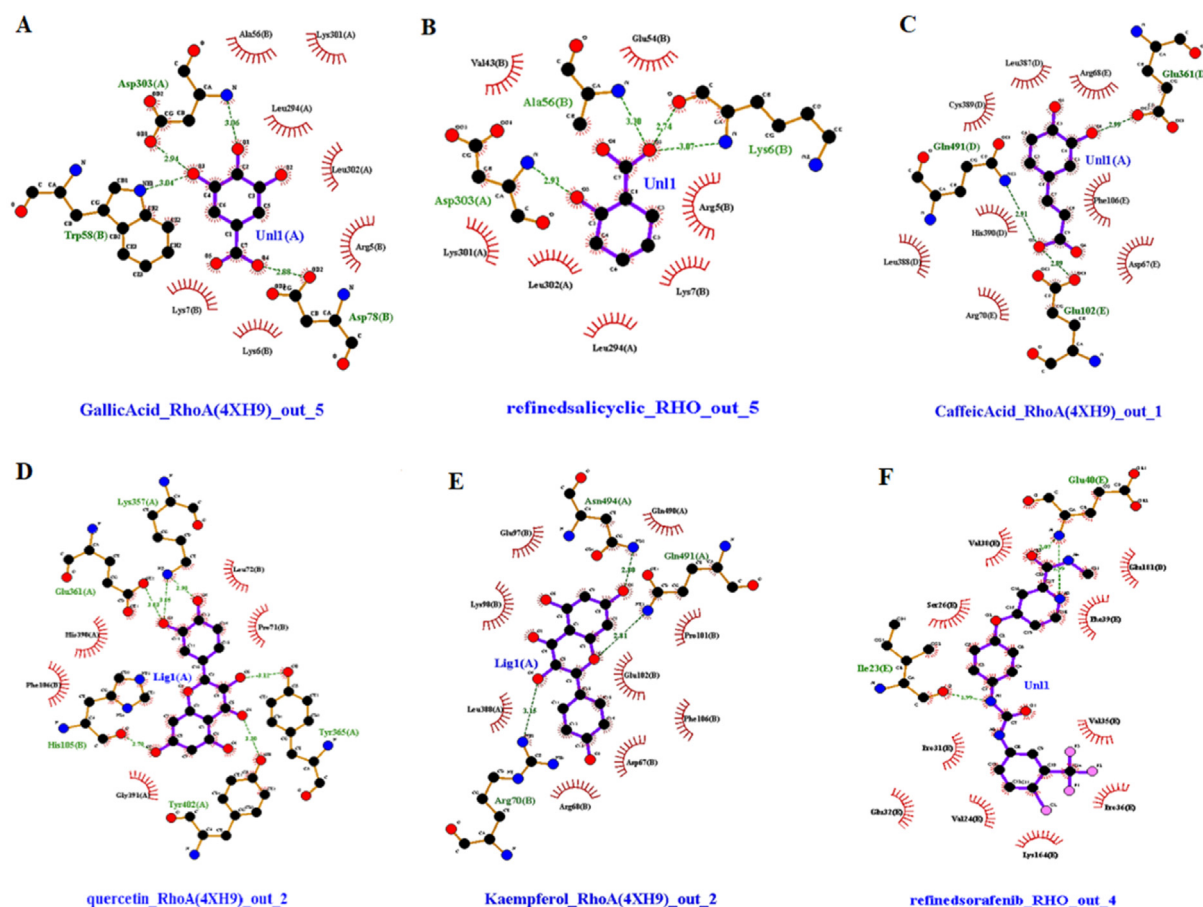


**Figure 5:** Ligplot Plus interaction results of the best-docked ligands with the target protein RhoA. Hydrogen bonds are shown as green dashed lines, and bond distances and hydrophobic interactions are indicated as spiked red arches. A presents the interaction between gallic acid and RhoA. B, C, D, and E present the interactions of salicylic acid, caffeic acid, quercetin, and kaempferol, respectively, with RhoA. F presents the interaction of the synthetic drug sorafenib with RhoA.

**Table 4: Molecular docking outcomes of ligands with target protein.**

No.	Ligand	Vina score kcal/mol	Cavity size	Molecular weight g/mol	Grid map	Maximum energy kcal/mol	Minimum energy kcal/mol
2	Gallic acid	-6.00	707	170.12	55	-3.49	-4.31
9	Quercetin	-8.20	1746	302.23	60	14.94	5.35
4	Caffeic acid	-6.10	2704	180.15	35	1.96	-4.22
1	Chlorogenic acid	-8.00	1746	354.31	60	22.88	9.89
5	Vanillic acid	-5.80	2704	168.14	55	9.65	3.86
12	Coumarin	-5.60	707	146.14	60	9.54	5.15
7	Sinapic acid	-5.60	2707	224.21	35	16.21	3.88
8	Ferulic acid	-5.80	1746	184.18	60	14.42	5.44
10	Salicylic acid	-5.60	707	138.12	60	5.61	2.96
11	Rutin	-9.70	2704	610.52	35	39.58	-2.95
6	Kaempferol	-7.90	1746	286.23	60	21.76	6.40
3	HB acid	-9.30	2704	614.16	24	70.34	9.46
	Sorafenib	-8.70	734	464.83	60	5.25	-20.31

kaempferol, quercetin, chlorogenic acid, and caffeic acid, were not confirmed to be CYP2D6 substrates.

Understanding a drug's complete clearance is essential to calculate dosage rates. On the basis of comparison to the reference drug, quercetin, kaempferol, gallic acid, salicylic acid, and caffeic acid showed high overall clearance. The

renal OCT2 substrate characteristic was absent from all chosen compounds. Similarly, a medicine's dose tolerance limit can be determined by understanding the toxicity of a selected ligand.<sup>41</sup> The chemicals chosen for this study, such as gallic acid and caffeic acid, were determined to be far safer for humans than the synthetic drug and the other two

**Table 5: Interaction of the target protein with selected ligands and the synthetic drug sorafenib, determined in Ligplot Plus software.**

No.	Ligand or drug	Binding energy (kcal/mol)	Number of hydrogen bonds	Amino acids	HBS distance	Hydrophobic interactions
10	Salicylic acid	-5.60	4	3	3.07 2.74 3.30 2.93	Glu54 Arg5 Lys7 Leu294 Leu302 Lys301 Val43
9	Quercetin	-8.20	6	5	3.03 3.05 2.98 2.70 3.30 3.12	Leu72 Pro71 Gly391 Phe 106 His 390
2	Gallic acid	-6.00	4	3	3.06 2.94 3.04 2.88	Lys301 Ala56 Leu294 Leu302 Arg5 Lys6 Lys7
6	Kaempferol	-7.90	3	3	2.80 2.81 3.15	Gln490 Pro101 Glu102 Phe106 Asp67 Arg68 Leu388 Lys98 Glu97
4	Caffeic acid	-6.10	3	3	2.89 2.91 2.99	Arg68 Leu387 Cys 389 Leu388 His 390 Arg 70 Asp67 Phe106
	Sorafenib	-8.70	1	2	2.99 3.07 2.99	Glu181 Phe39 Val35 Pro36 Lys164 Val124 Glu32 Pro31 Ser 26 Val38

selected ligands. Whereas the reference drug sorafenib itself showed hERG II inhibitory properties, no chosen drugs were found to be hERG I and hERG II inhibitors. The reference drug had greater oral rat acute toxicity than the other chosen ligands, such as gallic acid, salicylic acid, and caffeic acid. The chosen ligands had greater oral rat chronic toxicity (1.198) than sorafenib. Therefore, the synthetic drug was found to be more harmful than the chosen ligands. In an examination of hepatotoxicity, quercetin, gallic acid, and caffeic acid were not found to have any toxic effects. However, the reference drug showed hepatotoxicity. No selected ligands exhibited any adverse

reactions, whereas sorafenib, the synthetic drug, displayed some allergic reactions.

#### *Structure retrieval and virtual screening for MD simulation*

The RhoA protein's 3D structure was retrieved and modified by cleaning, energy minimization, and modeling. Notably, the protein has a length of 193 amino acids and only one domain: a small GTP-binding protein domain. Likewise, the ligand structures (salicylic acid, gallic acid, and caffeic acid) were generated in pdb format. The complexes with the highest binding affinity for each ligand were selected

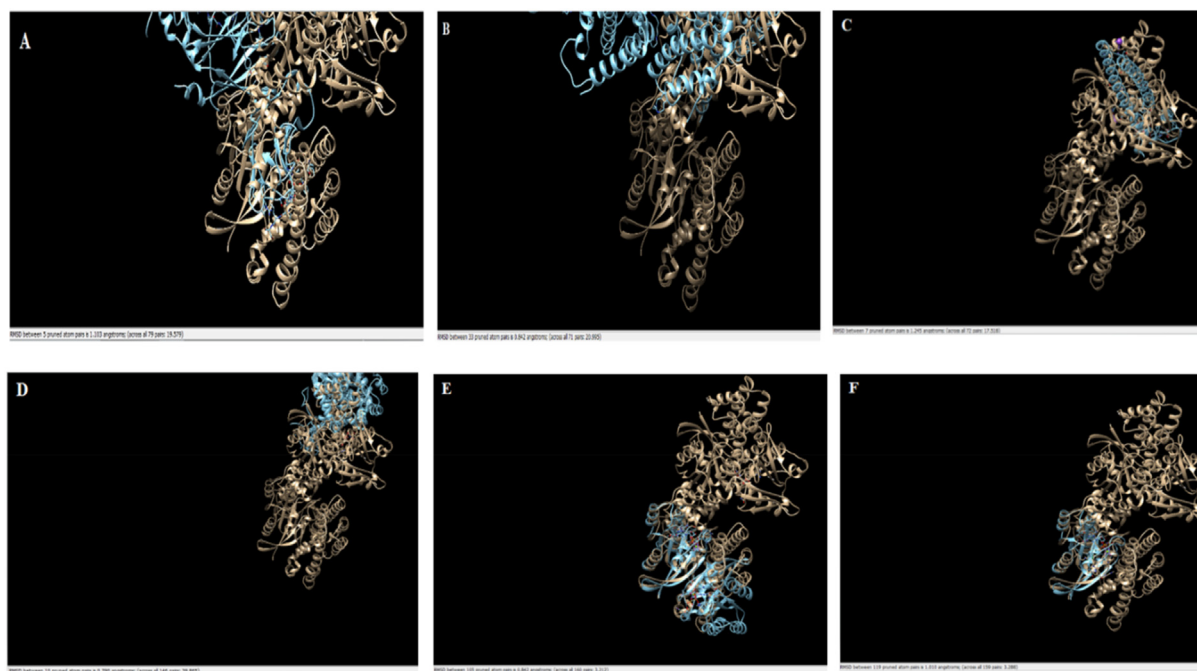


**Figure 6:** Best poses for RMSD values of selected ligands, determined with UCSF Chimera. Image A is the best pose, according to the RMSD value of gallic acid's interaction with RhoA. Images B, C, D, and E depict the best poses for salicylic acid, caffeic acid, quercetin, and kaempferol, respectively, with RhoA. Image F presents the interaction of the synthetic drug sorafenib with RhoA.

**Table 6: RMSD values of ligands (five poses) selected for docking.**

No.	Ligand	Vina score (kcal/mol)	RMSD (pose 1)	RMSD (pose2)	RMSD (pose 3)	RSMD (pose 4)	RSMD (pose 5)
7	Salicylic acid	−5.60	1.30	0.84	1.03	1.09	0.98
9	Quercetin	−8.20	0.94	0.93	0.79	1.11	1.58
2	Gallic acid	−6.00	1.21	1.24	1.10	1.45	1.20
6	Kaempferol	−7.90	0.89	1.02	1.34	0.84	0.94
4	Caffeic acid	−6.10	0.97	0.75	1.28	0.93	1.12
	Sorafenib	−8.80	1.01	1.10	0.98	0.87	0.99

from the screening complexes. The complex containing salicylic acid showed a binding affinity of  $-5.44$  kcal/mol, whereas the complex containing gallic acid showed a binding affinity of  $-6.01$  kcal/mol, and the complex containing caffeic acid showed a binding affinity of  $-6.11$  kcal/mol. According to our findings, caffeic acid had the highest binding affinity toward RhoA protein.

#### Interaction analysis of screened complexes

To emphasize the connections and to pinpoint the interacting residues between the ligands and the RhoA protein, we performed interaction analysis on the top complexes (Figures 7 and 8). The protein showed interactions with caffeic acid at residues CYS (159), ASN (117), ALA (161), and LYS (118). With the exception of ALA (161), every interaction occurred inside the small.

GTP-binding protein domain (5–159). The interactions were observed at residues SER (73) and ARG (70) in salicylic acid. Likewise, interactions were observed between gallic acid and residues ARG (70), PRO (71), and SER

(73). Within the small GTP-binding protein domain (5–159), both ligands interacted in every interaction. Table 5 lists the interactions between proteins and ligands, along with the associated residues and domains. Figure 8 shows the 2D and 3D protein-ligand interactions of complexes.

#### MD simulations of screened complexes

The stability and flexibility of the leading complexes of gallic acid, salicylic acid, and caffeic acid were examined with MD simulations. During the simulation period, the protein displayed an equilibrium state from 50.10 ns to 59.20 ns with caffeic acid. After the simulation, the ligand and protein had RMSD values of  $4.36$  Å and  $3.17$  Å, respectively. In addition, the protein and ligand had a minimal RMSD difference of 9.10 ns.

Throughout the simulation period, the gallic acid complex had an equilibrium point that moved from 60.90 ns to 85.10 ns. The protein and ligand had a minimal RMSD difference of 3.50 ns. The ligand's and protein's RMSD

**Table 7: ADMET properties of selected ligands and the synthetic drug sorafenib.**

Drug likeliness properties	Ligand or drug					
	Gallic acid	Salicylic acid	Caffeic acid	Quercetin	Kaempferol	Sorafenib
Log P-value	0.501	1.090	1.195	1.988	2.282	5.549
Molecular weight (g/mol)	170.120	138.122	180.159	302.238	286.239	464.831
Hydrogen bond acceptors	4	2	3	7	6	4
Hydrogen bond donors	4	2	3	5	4	3
Bonds (rotatable)	1	1	2	1	1	5
Surface area (Å <sup>2</sup> )	67.135	57.545	74.381	122.108	117.313	185.111
Water solubility (log mol/L)	-2.560	-1.808	-2.330	-2.925	-3.040	-4.442
Caco-2 permeability (log Papp 10 <sup>-6</sup> cm/s)	-0.081	-1.151	0.634	0.925	0.032	0.278
Intestinal absorption (human) (% absorb)	43.374	83.887	69.407	77.207	74.290	83.628
Skin permeability (log Kp)	-2.735	-2.723	-2.722	-2.735	-2.735	-3.037
P-glycoprotein substrate	No	No	No	Yes	Yes	Yes
P-glycoprotein I inhibitor	No	No	No	No	No	Yes
P-glycoprotein II inhibitor	No	No	No	No	No	No
VDss (human) (log L/kg)	-1.855	-1.570	-1.098	1.559	1.274	0.199
Fraction unbound (human) (Fu)	0.617	0.563	0.529	0.206	0.178	0.059
CNS permeability (log PS)	-3.740	-3.210	-2.608	-3.065	-2.228	-2.007
BBB permeability (log BB)	-1.102	-0.334	0.647	-1.098	-0.939	-1.684
CYP2D6 substrate	No	No	No	No	No	No
CYP 3A4 inhibitor	No	No	No	No	No	Yes
CYP1A2 inhibitor	No	No	No	Yes	Yes	Yes
CYP2C19 inhibitor	No	No	No	No	No	No
CYP2C9 inhibitor	No	No	No	No	No	Yes
CYP2D6 inhibitor	No	No	No	No	No	Yes
CYP3A4 inhibitor	No	No	No	No	No	Yes
Total clearance (log ml/min/kg)	0.718	0.607	0.508	0.407	0.477	-0.219
Renal OCT2 substrate	No	No	No	No	No	No
Ames toxicity	No	No	No	No	No	No
Maximum tolerated dose (human) (log mg/kg/day)	0.700	0.610	1.141	0.499	0.531	0.549
Herg I inhibitor	No	No	No	No	No	No
Herg II inhibitor	No	No	No	No	No	Yes
Oral rat acute toxicity (LD <sub>50</sub> ) (mol/kg)	2.218	2.282	2.383	2.471	2.449	2.788
Oral rat chronic toxicity (LOAEL) (log mg/kg_bw/day)	3.060	2.483	2.092	2.612	2.505	1.198
Hepatotoxicity	No	No	No	No	No	Yes
Skin sensitization	No	No	No	No	No	Yes
Minnow toxicity (log Mm)	3.188	1.812	2.246	3.721	2.885	0.189

values at the conclusion of the simulation were 17.43 Å and 6.38 Å, respectively. Finally, the protein showed an equilibrium state with salicylic acid between 83.80 and 98.20 ns, whereas the ligand and protein's RMSD values at the end of the simulation period ranged from 5.37 to 32.54 Å. The protein and ligand had a minimal RMSD difference of 8.50 ns.

The caffeic acid-RhoA complex, in contrast, had the lowest RMSD, thereby indicating that caffeic acid binding imparts stability to the protein complex. Gallic acid and salicylic acid binding to RhoA showed higher RMSD values, thus indicating less specific binding interactions for these ligands than caffeic acid. These findings suggested that the conformations of the complexes formed with gallic acid and salicylic acid might show more noticeable changes or fluctuations during binding, thus potentially indicating weaker binding to the RhoA protein than observed with caffeic acid. Figure 9 (A) shows the RMSD plots of all proteins with their top-scoring compounds.

RMSF is used to characterize localized changes along protein chains. The peaks in the plot indicated areas of the protein showing fluctuations during the simulation period. Almost all complexes displayed similar patterns in the RMSF plots

(Figure 9 (B)). The complexes of caffeic acid and salicylic acid bound to RhoA fluctuated in the range of 1–3.00 Å, whereas gallic acid fluctuated in the range of 1–4.50 Å. The tail region (C-terminus and N-terminus) of the protein showed more fluctuations than the residue on the binding site.<sup>42</sup> In MD simulations, a higher RMSF value indicates that the complex undergoes substantial variation; consequently, a lower RMSF reflects fewer flexibility changes and implies a more stable region within the structure.<sup>43</sup> Our findings suggested that caffeic acid bound RhoA in distinct patterns remained mostly stable during the simulation period. Among all three complexes, the gallic acid complex displayed a slightly higher RMSF value and therefore might be more flexible than the other two complexes.

Compared with salicylic acid and caffeic acid, gallic acid had a markedly higher polar surface area, thereby suggesting a greater potential for polar interactions, such as hydrogen bonding, and promoting stability (Figure 10 A). However, compared with gallic acid and salicylic acid, caffeic acid had a significantly lower SASA value, thus suggesting that the molecule became either less stretched or more compact (Figure 10 B). Finally, caffeic acid displayed the greatest radius of gyration (Figure 10C), thereby suggesting a less

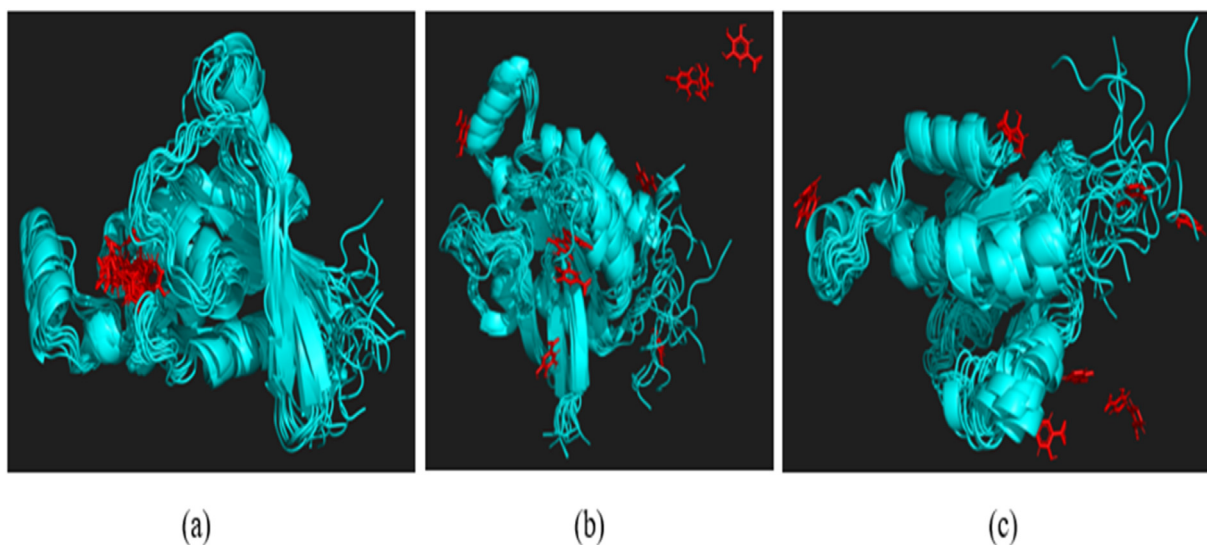


**Figure 7:** MD simulation results. (a–c) Comparative visualization of trajectories of the caffeic acid-RhoA, gallic acid-RhoA, and salicylic acid-RhoA complexes, respectively.

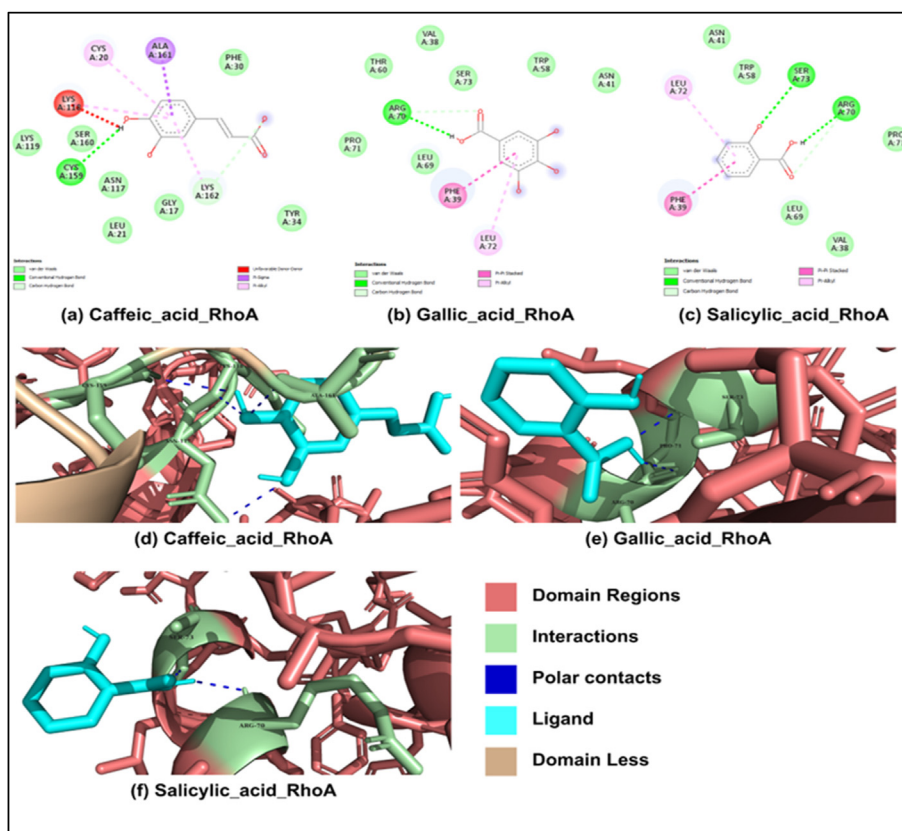


**Figure 8:** Interaction analysis of protein-ligand complexes. (a–c) 2D illustration of interactions of key residues in RhoA protein binding pockets with ligands during 100 ns MD simulations. (d–f) 3D illustration of interactions of RhoA protein with ligands within domain regions.

compact or more elongated molecule with decreased stability as a result of increased flexibility.

Our findings suggested that caffeic acid might have had the greatest ability to inhibit the RhoA protein, because it remained bound to the protein structure and intact throughout the simulation run, thereby demonstrating a

robust interaction between the ligand and the protein and suggesting a possible inhibitory effect. However, the other ligands, gallic acid, and salicylic acid, did not remain intact and bound to the protein structure over the simulation run, thereby indicating weak binding to the protein. Several plant phytochemicals have been investigated in

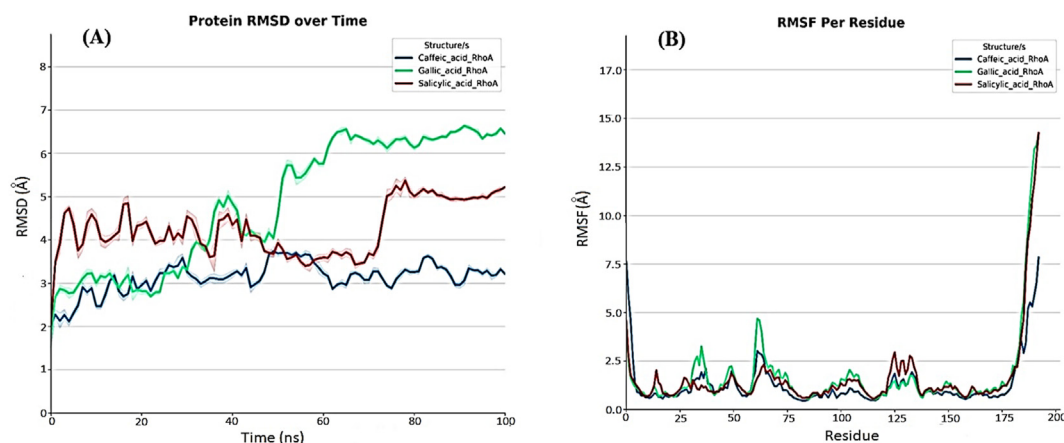


**Figure 9:** RMSD fluctuation of protein backbones during the MD simulation (A). MD simulation depicting the RMSF plot per residue for RhoA protein in complex with ligands. In the RMSF plot, the peaks indicate the protein areas fluctuating the most during simulation (B).

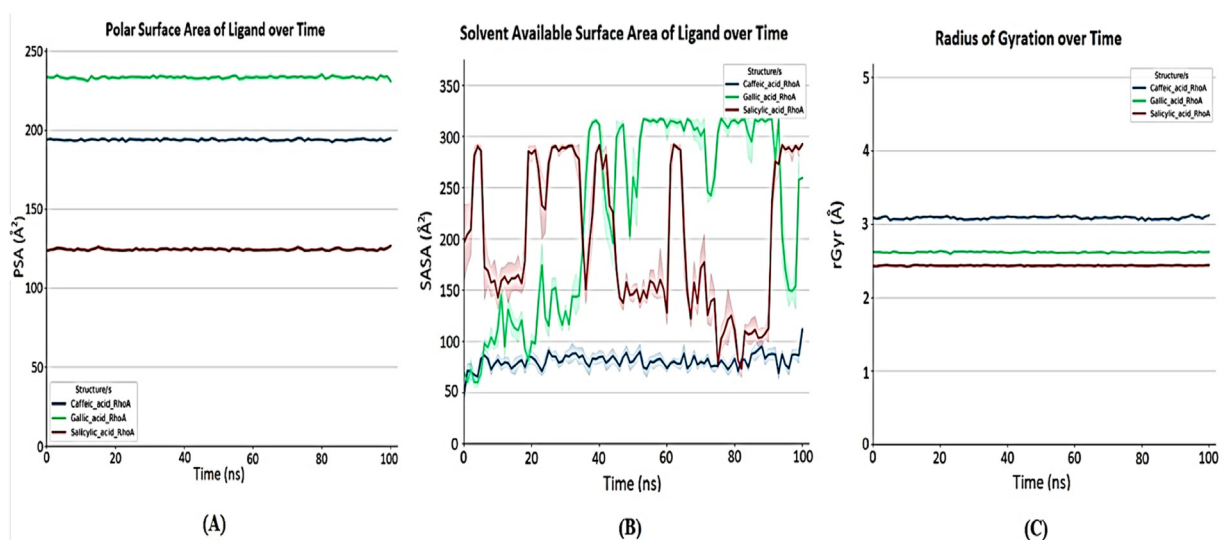


**Figure 10:** MD simulation results depicting ligand properties, including polar surface area (A), solvent available surface area (B), and radius of gyration (C).

HCC through *in silico* approaches, such as molecular docking and MD simulation.<sup>44</sup> Another study has used molecular docking techniques to examine the activity of leaf extracts of *Inula viscosa* against human liver cancer cells.<sup>45</sup>

#### Comparison of lead compounds versus the selected drug

To determine the lead compound, we compared the standard drug and selected ligands according to aspects such as interaction properties, docking values, and ADMET properties (RMSD and RMSF values). We anticipated from the data analysis that the selected ligands, salicylic acid, gallic acid, and caffeic acid, would be possible drug candidates. Caffeic acid was considered the best lead compound for multiple reasons: it followed Lipinski's rule of five, and it had favorable ADMET

properties, good intestinal absorption, water solubility, skin permeability, and safety. Furthermore, it showed stability throughout the MD simulation run, with low RMSD and RMSF values, and significantly lower SASA values than the other candidates. Given that caffeic acid was the most stable and the safest compound for humans, and that it had the lowest RMSD value during the MD simulation, thus indicating that its binding imparts stability, this compound might be a viable option for future medication development.

Additionally, caffeic acid was expected to have the highest binding affinity toward RhoA protein during MD simulation. Caffeic acid is a polyphenol that is found in plants, and has antioxidant and anticancer properties.<sup>46</sup> Another study has indicated that caffeic acid can effectively treat cervical cancer through two distinct pathways; therefore, this compound has the potential to fight cancer in combination

with other substances.<sup>47</sup> Research on the medicinal properties of caffeic acid has revealed that this compound prevents cell invasion and migration, and might even lessen the spread of cancer.<sup>48</sup> Caffeic acid plays an important role in combatting liver cancer: many *in vivo* and *in vitro* studies have found that this compound inhibits hepatic carcinoma through various mechanisms including cell death and activation of caspase 9.<sup>49</sup> Therefore, in the future, caffeic acid, the lead compound, might be considered as a promising therapeutic candidate to target Rho GTPases, specifically RhoA. Epigallocatechin a polyphenol is a type of catechin that suppresses RhoA signaling in human hepatic stellate cell lines.<sup>50</sup>

Dysregulation of the RhoA gene has been studied in HCC<sup>51</sup> and might serve as a possible therapeutic target. Moreover, many studies have shown that upregulation of RhoA enhances the migration of cells of HCC. For example, RhoA/ROCK activates by upregulation of supervillin by hypoxia-induction, thereby activating the protein kinase (ERK)/p38 pathway, and promoting the migration and invasion of HCC cells.<sup>52</sup> RhoA/ROCK also modifies the ECM in the tumor microenvironment and consequently promotes the invasion of HCC cells.<sup>53</sup> RhoA prevents apoptosis in HCC cells by RTKN, which helps activate NF- $\kappa$ B signaling. Furthermore, RhoA blocks apoptosis of HCC cells by Rock2, whenever activated by ECT2.<sup>54</sup> Moreover, *H. rhamnoides* extract and its iron oxide nanoparticles have been found to be effective in downregulating RhoA gene expression in the liver cancer cell line HePG2 and therefore might be a suitable drug target for liver cancer treatment.<sup>55</sup> A previous study has investigated the therapeutic effects of several bioactive compounds from plants against HCC through *in silico* approaches.<sup>56</sup> In another study, polyphenols from seedless black grapes (*Vitis vinifera*) have shown potential cytotoxic activity against the Hep G2 and Huh7 cell lines.<sup>57</sup>

## Conclusion

This study assessed the anticancer potential of *H. rhamnoides* polyphenols in liver cancer by focusing on the RhoA gene. Through HPLC chromatography, 12 polyphenols were found in the methanolic extract of *H. rhamnoides*. On the basis of the Vina score, grid map score, and cavity size, five polyphenols were chosen for additional research with *in silico* techniques such as molecular docking. By considering ADMET properties, and RMSD and RMSF values, we compared the polyphenols quercetin, kaempferol, gallic acid, salicylic acid, and caffeic acid with the standard drug sorafenib. When choosing the ligands to investigate further as a potential lead compound, we used Lipinski's rule of five. Among the chosen ligands, caffeic acid was determined to be the most promising medication candidate, because of its excellent ADMET characteristics, and docking and MD simulation results. Taking into account all the aforementioned characteristics, we determined that caffeic acid might be a viable future therapeutic option to treat liver cancer by targeting the RhoA gene.

## Source of funding

This research did not receive any specific grant from funding agencies in the public, commercial, or not-for-profit sectors.

## Conflict of interest

The authors have no relevant financial or non-financial interests to disclose.

## Ethical approval

The authors report no ethical issues.

## Authors' contributions

All authors contributed to the study conception and design. R.T. performed all research and wrote the first draft of the article. E.D. supervised all research and proofread the article. All authors read and approved the final manuscript. All authors have critically reviewed and approved the final draft and are responsible for the content and similarity index of the manuscript.

## Acknowledgments

We are grateful to the Capital University of Science and Technology Islamabad for providing us with a platform to conduct this research.

## References

1. Tahtabasi M, Mohamud Abdullahi I, Kalayci M, Gedi Ibrahim I, Er S. Cancer incidence and distribution at a Tertiary Care Hospital in Somalia from 2017 to 2020: an initial report of 1306 cases. *Cancer Management and Research*; 2020. pp. 8599–8611.
2. Hanahan D, Weinberg RA. The hallmarks of cancer. *Cell* 2000; 100(1): 57–70.
3. Zamarin D, Holmgaard RB, Subudhi SK, Park JS, Mansour M, Palese P, et al. Localized oncolytic virotherapy overcomes systemic tumor resistance to immune checkpoint blockade immunotherapy. *Sci Transl Med* 2014; 6(226). 226ra32-ra32.
4. Siegel R, Miller K, Jemal RA. Cancer facts & figures 2021. In: *CABI*. American Cancer Society. Inc; 2021. 20210059750, <https://www.cabidigitallibrary.org/doi/full/10.5555/20210059750>.
5. Center MM, Jemal A. International trends in liver cancer incidence rates. *Cancer Epidemiol Biomarkers Prev* 2011; 20(11): 2362–2368.
6. Anwanwan D, Singh SK, Singh S, Saikam V, Singh R. Challenges in liver cancer and possible treatment approaches. *Biochim Biophys Acta Rev Cancer* 2020; 1873(1):188314.
7. Orgaz JL, Herraiz C, Sanz-Moreno V. Rho GTPases modulate malignant transformation of tumor cells. *Small GTPases* 2014; 5(4):e983867.
8. Jansen S, Gosens R, Wieland T, Schmidt M. Paving the Rho in cancer metastasis: Rho GTPases and beyond. *Pharmacol Therapeut* 2018; 183: 1–21.

9. Wang T, Rao D, Yu C, Sheng J, Luo Y, Xia L, Huang W. RHO GTPase family in hepatocellular carcinoma. **Exp Hematol Oncol** 2022; 11(1): 91.
10. Chang HR, Nam S, Lee J, Kim J-H, Jung HR, Park HS, et al. Systematic approach identifies RHOA as a potential biomarker therapeutic target for Asian gastric cancer. **Oncotarget** 2016; 7(49):81435.
11. Makarem N, Bandera EV, Nicholson JM, Parekh N. Consumption of sugars, sugary foods, and sugary beverages in relation to cancer risk: a systematic review of longitudinal studies. **Annu Rev Nutr** 2018; 38: 17–39.
12. Smitha Grace S, Chandran G, Chauhan JB. *Terpenoids: an activator of “fuel-sensing enzyme AMPK” with special emphasis on antidiabetic activity. Phytochemistry and Molecular Aspects*. Springer International Publishing; 2019. pp. 227–244.
13. Yadav A, Stobdan T, Chauhan O, Dwivedi S, Chaurasia O. Sea buckthorn: a multipurpose medicinal plant from upper Himalayas. **Med Plants: From Farm to Pharmacy** 2019: 399–426. Springer, Cham.
14. Oomah BD. Sea buckthorn lipids. In: Li TSC, Beveridge T, editors. *Sea buckthorn (Hippophae rhamnoides): Production and utilization*. Ottawa, ON: NRC Research Press; 2003. pp. 51–68.
15. Sahoo R, Pattanaik S, Pattnaik G, Mallick S, Mohapatra R. Review on the use of molecular docking as the first line tool in drug discovery and development. **Indian J Pharmaceut Sci** 2022; 84(5).
16. Pinzi L, Rastelli G. Molecular docking: shifting paradigms in drug discovery. **Int J Mol Sci** 2019; 20(18): 4331.
17. Bouaouich A, Bouguerche F. HPLC Chromatographic Analysis Antioxidant activity of seeds some varieties of prickly pear (*Opuntia ficus-indica* L.) from the Sidi-Fredj souk Ahras Algeria. **Algerian Journal of Biosciences** 2022; 3(1): 38–46.
18. Foddai M, Maldini M, Addis R, Petretto GL, Chessa M, Pintore G. Profiling of the bioactive compounds in flowers, leaves and roots of *Vinca sardoa*. **Nat Prod Commun** 2017; 12(6):1934578X1701200625.
19. Kim S. Exploring chemical information in PubChem. **Current Protocols** 2021; 1(8): e217.
20. Ralte L, Khiangte L, Thangjam NM, Kumar A, Singh YT. GC–MS and molecular docking analyses of phytochemicals from the underutilized plant, *Parkia timoriana* revealed candidate anti-cancerous and anti-inflammatory agents. **Sci Rep** 2022; 12(1): 3395.
21. Liu Y, Yang X, Gan J, Chen S, Xiao Z-X, Cao Y. CB-Dock2: improved protein–ligand blind docking by integrating cavity detection, docking and homologous template fitting. **Nucleic Acids Res** 2022; 50(W1): W159–W164.
22. Margaretha F, Subagja M, Putri AD, Salam CQ, Valenthenardo L, Adhiwijaya PK, et al. Comprehensive analysis of protein-protein interactions (PPIs) with structure prediction program for breast cancer determination. **Berkala Penelitian Hayati** 2023; 29(3): 87–94.
23. McNutt AT, Francoeur P, Aggarwal R, Masuda T, Meli R, Ragoza M, et al. GNINA 1.0: molecular docking with deep learning. **J Cheminf** 2021; 13(1): 43.
24. Abdelmoniem NH, Abdallah MM, Mukhtar R, Moutasim F, Rafie Ahmed A, Edris A, et al. Identification of novel natural dual HDAC and Hsp90 inhibitors for metastatic TNBC with e-pharmacophore modeling, molecular docking, and molecular dynamics studies. **Molecules** 2023; 28(4): 1771.
25. Criste A, Urcan AC, Bunea A, Pripon Furtuna FR, Olah NK, Madden RH, Corcionivoschi N. Phytochemical composition and biological activity of berries and leaves from four Romanian sea buckthorn (*Hippophae rhamnoides* L.) varieties. **Molecules** 2020; 25(5): 1170.
26. Ficzek G, Mátravölgyi G, Furulyás D, Rentsendavaa C, Jöcsák I, Papp D, et al. Analysis of bioactive compounds of three sea buckthorn cultivars (*Hippophae rhamnoides* L. ‘Askola’, ‘Leikora’, and ‘Orangeveja’) with HPLC and spectrophotometric methods. **Eur J Hort Sci** 2019; 84(1): 31–38.
27. Arimboor R, Kumar KS, Arumughan C. Simultaneous estimation of phenolic acids in sea buckthorn (*Hippophae rhamnoides*) with RP-HPLC with DAD. **J Pharmaceut Biomed Anal** 2008; 47(1): 31–38.
28. Nahar J, Boopathi V, Murugesan M, Rupa EJ, Yang DC, Kang SC, Mathiyalagan R. Investigating the anticancer activity of G-Rh1 with in silico and in vitro studies (A549 lung cancer cells). **Molecules** 2022; 27(23): 8311.
29. Ajjarapu SM, Tiwari A, Taj G, Singh DB, Singh S, Kumar S. Simulation studies, 3D QSAR and molecular docking on a point mutation of protein kinase B with flavonoids targeting ovarian Cancer. **BMC Pharmacology and Toxicology** 2021; 22: 1–23.
30. Clayton NS, Ridley AJ. Targeting Rho GTPase signaling networks in cancer. **Front Cell Dev Biol** 2020; 8: 222.
31. Murumkar PR, Sharma MK, Gupta P, Patel NM, Yadav MR. Selection of suitable protein structure from protein data bank: an important step in structure-based drug design studies. **Mini Rev Med Chem** 2023; 23(3): 246–264.
32. Sindhu HA, Afzal M, Shahid I. Pharmacological activities and in-silico studies of bioactive compounds identified in organic fractions of the methanolic extract of *Citrullus colocynthis*. **Dose Response** 2023; 21(3). 15593258231187357.
33. Iwaloye O, Ottu PO, Olawale F, Babalola OO, Elekofehinti OO, Kikiowo B, et al. Computer-aided drug design in anti-cancer drug discovery: what have we learnt and what is the way forward? **Inform Med Unlocked** 2023; 41:101332.
34. Liu Y, Grimm M, Dai W-t, Hou M-c, Xiao Z-X, Cao Y. CB-Dock: a web server for cavity detection-guided protein–ligand blind docking. **Acta Pharmacol Sin** 2020; 41(1): 138–144.
35. Gurung AB, Ali MA, Lee J, Farah MA, Al-Anazi KM. Molecular docking and dynamics simulation study of bioactive compounds from *Ficus carica* L. with important anticancer drug targets. **PLoS One** 2021; 16(7):e0254035.
36. Shoaib TH, Abdelmoniem N, Mukhtar RM, Alqhtani AT, Alalawi AL, Alawaji R, et al. Molecular docking and molecular dynamics studies reveal the anticancer potential of medicinal-plant-derived lignans as MDM2-P53 interaction inhibitors. **Molecules** 2023; 28(18): 6665.
37. Yugandhar P, Kumar KK, Neeraja P, Savithramma N. Isolation, characterization and in silico docking studies of synergistic estrogen receptor a anticancer polyphenols from *Syzygium alternifolium* (Wt.) Walp. **Journal of Intercultural Ethnopharmacology** 2017; 6(3): 296.
38. Pollastri MP. Overview on the rule of five. **Curr Protoc Pharmacol** 2010; 49(1): 9.12. 1–9.9. 8.
39. Aziz NA, George RF, El-Adl K, Mahmoud WR. Design, synthesis, in silico docking, ADMET and anticancer evaluations of thiazolidine-2, 4-diones bearing heterocyclic rings as dual VEGFR-2/EGFR T790M tyrosine kinase inhibitors. **RSC Adv** 2022; 12(20): 12913–12931.
40. Olaokun OO, Zubair MS. Antidiabetic activity, molecular docking, and ADMET properties of compounds isolated from bioactive ethyl acetate fraction of *Ficus lutea* leaf extract. **Molecules** 2023; 28(23): 7717.
41. Dali Y, Abbasi SM, Khan SAF, Larra SA, Rasool R, Ain QT, Jafar TH. Computational drug design and exploration of potent phytochemicals against cancer through in silico approaches. **Biomed Lett** 2019; 5(1): 21–26.
42. Zare F, Ataollahi E, Mardaneh P, Sakhteman A, Keshavarz V, Solhjoo A, Emami L. A combination of virtual screening, molecular dynamics simulation, MM/PBSA, ADMET, and DFT calculations to identify a potential DPP4 inhibitor. **Sci Rep** 2024; 14(1): 7749.
43. Oyewusi HA, Wahab RA, Akinyede KA, Albadrani GM, Al-Ghadi MQ, Abdel-Daim MM, et al. Bioinformatics analysis

- and molecular dynamics simulations of azoreductases (AzrBmH2) from *Bacillus megaterium* H2 for the decolorization of commercial dyes. **Environ Sci Eur** **2024**; 36(1): 31.
44. Mustafa G, Younas S, Mahrosh HS, Albeshr MF, Bhat EA. Molecular docking and simulation-binding analysis of plant phytochemicals with the hepatocellular carcinoma targets epidermal growth factor receptor and caspase-9. **Molecules** **2023**; 28(8): 3583.
  45. Kheyar-Kraouche N, Boucheffa S, Bellik Y, Farida K, Brahmi-Chendouh N. Exploring the potential of *Inula viscosa* extracts for antioxidant, antiproliferative and apoptotic effects on human liver cancer cells and a molecular docking study. **Bio-technologie** **2023**; 104(2): 183.
  46. Birková A, Hubková B, Bolerázská B, Mareková M, Čizmarová B. Caffeic acid: a brief overview of its presence, metabolism, and bioactivity. **Bioactive Compounds in Health and Disease-Online ISSN: 2574-0334; Print ISSN: 2769-2426** **2020**; 3(4): 74–81.
  47. Tyszká-Czochara M, Konieczny P, Majka M. Caffeic acid expands anti-tumor effect of metformin in human metastatic cervical carcinoma HTB-34 cells: implications of AMPK activation and impairment of fatty acids de novo biosynthesis. **Int J Mol Sci** **2017**; 18(2): 462.
  48. Weng C-J, Yen G-C. Chemopreventive effects of dietary phytochemicals against cancer invasion and metastasis: phenolic acids, monophenol, polyphenol, and their derivatives. **Cancer Treat Rev** **2012**; 38(1): 76–87.
  49. Espíndola KMM, Ferreira RG, Narvaez LEM, Silva Rosario ACR, Da Silva AHM, Silva AGB, et al. Chemical and pharmacological aspects of caffeic acid and its activity in hepatocarcinoma. **Front Oncol** **2019**; 9: 541.
  50. Higashi N, Kohjima M, Fukushima M, Ohta S, Kotoh K, Enjoji M, et al. Epigallocatechin-3-gallate, a green-tea polyphenol, suppresses Rho signaling in TWNT-4 human hepatic stellate cells. **J Lab Clin Med** **2005**; 145(6): 316–322.
  51. Bai Y, Xie F, Miao F, Long J, Huang S, Huang H, et al. The diagnostic and prognostic role of RhoA in hepatocellular carcinoma. **Aging (Albany NY)** **2019**; 11(14): 5158.
  52. Du Y, Lu S, Ge J, Long D, Wen C, Tan S, et al. ROCK2 disturbs MKP1 expression to promote invasion and metastasis in hepatocellular carcinoma. **Am J Cancer Res** **2020**; 10(3): 884.
  53. Sun C, Hu A, Wang S, Tian B, Jiang L, Liang Y, et al. ADAM17-regulated CX3CL1 expression produced by bone marrow endothelial cells promotes spinal metastasis from hepatocellular carcinoma. **Int J Oncol** **2020**; 57(1): 249–263.
  54. Xu C, Wan X, Xu L, Weng H, Yan M, Miao M, et al. Xanthine oxidase in non-alcoholic fatty liver disease and hyperuricemia: one stone hits two birds. **J Hepatol** **2015**; 62(6): 1412–1419.
  55. Tabassum R, Dilshad E. A comparative anticancer analysis of iron oxide nanoparticles of *Hippophae rhamnoides* and *Cichorium intybus* found in the Karakoram Range of Gilgit Baltistan against liver cancer targeting the RhoA gene. **Drug Dev Ind Pharm** **2024**; 1–14 (in press).
  56. Rai D, George S. Computational analysis of ligands from natural products on the cellular targets of combined hepatocellular carcinoma and cholangiocarcinoma. **Nat Prod Res** **2024**; 1–9.
  57. Shaban NZ, Hegazy WA, Abu-Serie MM, Talaat IM, Awad OM, Habashy NH. Seedless black *Vitis vinifera* polyphenols suppress hepatocellular carcinoma in vitro and in vivo by targeting apoptosis, cancer stem cells, and proliferation. **Biomed Pharmacother** **2024**; 175:116638.

**How to cite this article:** Tabassum R, Dilshad E. *In silico* screening of *Hippophae rhamnoides* polyphenols targeting the RhoA protein as a potential liver cancer treatment. **J Taibah Univ Med Sc** **2025**;20(1):89–106.